

1 **Significant Increase in Atlantic Ocean Heat Content Since the mid-20th**
2 **Century**

3
4
5
6
7 Sang-Ki Lee^{1,2}, Wonsun Park³, Erik van Sebille⁵, Chunzai Wang², David B. Enfield^{1,2}, Steven
8 Yeager⁴, Ben Kirtman⁵, and Molly Baringer²

9 ¹CIMAS, University of Miami, Miami, Florida, USA

10 ²AOML, NOAA, Miami Florida, USA

11 ³IFM-GEOMAR, Kiel, Germany

12 ⁴NCAR, Boulder, Colorado, USA

13 ⁵RSMAS, University of Miami, Miami, Florida, USA

14
15
16 April 2011

17
18
19
20
21
22 Corresponding author: Dr. Sang-Ki Lee (Sang-Ki.Lee@noaa.gov).

1 **The Atlantic Ocean has warmed substantially more than any other ocean basin during**
2 **the later half of the 20th century. This paper proposes a hypothesis that the enhanced**
3 **warming in the Atlantic is largely due to the increased ocean heat transport into the**
4 **Atlantic basin across 30°S. A surface-forced global ocean-ice coupled model is used to test**
5 **this hypothesis and to further show that the anomalous ocean heat convergence in the**
6 **Atlantic Ocean is caused by the increased ocean heat transport from the Indian Ocean. The**
7 **increased wind stress curl over the region from 50°S to 30°S may have contributed to the**
8 **increased ocean heat transport from the Indian Ocean since the 1950s.**

9 Instrumental records indicate that the heat content of the Atlantic Ocean in the upper 3000 m
10 has substantially increased during the later half of the 20th century at a rate ($\sim 8 \times 10^{22}$ J per
11 40yrs) exceeding that of the Pacific Ocean ($\sim 4 \times 10^{22}$ J per 40yrs) and Indian Ocean ($\sim 3 \times 10^{22}$ J
12 per 40yrs) combined⁶, even though the Atlantic Ocean covers less than 20% of the global ocean
13 in surface area. This is also apparent in the recently updated estimates for the upper 700 m with
14 additional data and instrumental bias corrections⁸. Climate model experiments with and without
15 anthropogenic greenhouse forcing have shown that the observed warming of the global ocean
16 since the mid-20th century could be largely attributed to the anthropogenic greenhouse effect⁷.
17 However, a question still remains as to why the warming trend in the Atlantic Ocean is
18 substantially larger than that in other ocean basins. This is also an important question for our
19 understanding of past, present and future climate variability, particularly since recent studies
20 have shown that tropical precipitation and Atlantic hurricane activity in the 21st century could be
21 affected by a differential inter-basin ocean warming^{5,16}.

22 Deep convective mixing over the North Atlantic sinking regions could maintain the subpolar
23 North Atlantic sea surface temperatures (SSTs) relatively insensitive to the anthropogenic

1 greenhouse effect⁶, and thus decrease the longwave heat loss at the sea surface and increase the
2 radiative heating associated with anthropogenic greenhouse gases (back radiation – upward
3 longwave radiation). However, this hypothesis appears to be inconsistent with the observed
4 cooling trend of the subpolar North Atlantic Ocean in the upper 1500 m during the 1950s-1990s⁹.

5 Perhaps, the answer to this conundrum can be found in the global overturning circulation,
6 which carries ocean heat from the North Pacific to the North Atlantic via the Indian and South
7 Atlantic Oceans³. Assuming that the surface warming associated with the anthropogenic
8 greenhouse effect is more or less uniform over the global ocean, the ocean heat transport by the
9 global overturning circulation should increase as the upper ocean warms globally. The increased
10 ocean heat transport should further warm the Atlantic Ocean since the Atlantic basin is
11 characterized by advective heat convergence (i.e., the northward ocean heat transport at 30°S in
12 the South Atlantic is positive) due to the Atlantic Meridional Overturning Circulation (AMOC),
13 which is the Atlantic component of the global overturning circulation. The Atlantic warming
14 should continue, unless the AMOC weakens, until the deep ocean fully adjusts to the surface
15 warming and exports the warm water out of the basin at depth.

16 The observed warming trend during the later half of the 20th century is large in both North
17 and South Atlantic basins⁶. This indicates anomalous advective heat convergence in both the
18 South and North Atlantic basins, and thus suggests a larger increase in the ocean heat transport
19 into the South Atlantic at 30°S and a lesser increase into the North Atlantic. This also suggests
20 that the strength and spatial structure of the AMOC may have shifted. However, there is no
21 reliable long-term instrumental record for AMOC variability and the associated northward ocean
22 heat transport. It appears that an ocean model-based reconstruction is likely to be our best chance
23 for assessing the history of AMOC and associated northward ocean heat transport for the 20th

1 century because the observed surface flux fields, which constrain ocean-only (or ocean-ice
2 coupled) models, are available on relatively long time scales.

3 Figure 1a shows the simulated Atlantic Ocean heat content change in the upper 3000m in
4 reference to the 1871-1900 period obtained from the three model experiments, along with the
5 observed trend of the Atlantic Ocean heat content increase. The simulated heat content of the
6 Atlantic Ocean in EXP_CTR is increased slightly during the first half of the 20th century, after
7 which it increases substantially by $\sim 9 \times 10^{22}$ J between the 1950s and 1990s. This large increase
8 is surprisingly close to the observed Atlantic Ocean heat content increase of $\sim 8 \times 10^{22}$ J during
9 the same period⁶, suggesting that the model experiment reasonably well reproduces the heat
10 budget trend of the Atlantic Ocean after the 1950s. If the northward heat transport in the South
11 Atlantic at 30°S is fixed at its 1871-1900 level by considering the fully transient surface fluxes
12 only in the north of 30°S (EXP_ATL), the Atlantic Ocean heat content increase is only $\sim 2 \times 10^{22}$
13 J between the 1950s and 1990s, and thus cannot explain the observed Atlantic Ocean heat
14 content increase. On the other hand, if the northward heat transport in the South Atlantic at 30°S
15 is allowed to vary in real time by considering the fully transient surface fluxes in the south of
16 30°S while keeping the surface fluxes over the Atlantic Ocean at their 1871-1900 levels
17 (EXP_REM), the Atlantic Ocean heat content is increased by $\sim 8 \times 10^{22}$ J between the 1950s and
18 1990s almost matching the observed trend.

19 Figure 1b shows that, in both EXP_CTR and EXP_REM, the northward ocean heat transport
20 at 30°S in the South Atlantic is about 0.1 PW larger in the 1950s - 1990s than in the earlier
21 periods, consistent with the large Atlantic Ocean heat content increases in these cases. In the case
22 of EXP_ATL, the increase is very small, also consistent with the small Atlantic Ocean heat
23 content increase for this case. Therefore, these model results fully support the hypothesis that the

1 enhanced warming of the Atlantic Ocean during the later half of the 20th century is largely due
2 to the increased ocean heat transport into the Atlantic basin across 30°S.

3 The next question is whether the increased upper ocean temperature in the South Atlantic at
4 30°S is sufficient to explain the large increase (~ 0.1 PW) in the simulated ocean heat transport
5 into the Atlantic basin. To answer this question, an additional model experiment, which is similar
6 to EXP_REM but without considering the surface wind change south of 30°S, is performed. This
7 model experiment suggests that the upper ocean thermal change of the inflow accounts for a
8 smaller portion (~ 30%) of the simulated ocean heat transport increase at 30°S in the South
9 Atlantic (not shown). Therefore, the baroclinic volume transport (i.e., AMOC) at 30°S is
10 explored next.

11 Figure 2a shows the time-averaged AMOC during 1979-2008 obtained from EXP_CTR. The
12 simulated maximum strength of the AMOC at 30°N is only 9 Sv ($1\text{Sv} = 10^6 \text{ m}^3\text{s}^{-1}$), which is
13 smaller than the observed range of 14 - 20Sv. Increasing the vertical diffusivity in the model
14 boosts the AMOC strength as shown in earlier studies. However, since other model features
15 deteriorate with the increased vertical diffusivity, the vertical diffusivity in the model is not
16 increased in this study. Despite the smaller maximum strength, the overall spatial structure of the
17 simulated AMOC is quite close to that derived from observations¹⁰.

18 Figure 2b shows the time series of the simulated AMOC index (maximum overturning
19 stream function) at 30°S. It clearly shows that the AMOC at 30°S increases after the 1950s,
20 suggesting that the increased northward heat transport in the South Atlantic at 30°S (Figure 1b) is
21 not only caused by the increased upper ocean temperature at 30°S but also by the increased
22 AMOC at 30°S. The AMOC at 30°S in EXP_REM has a similar increase as in EXP_CTR
23 (Figure S1a). On the other hand, the AMOC at 30°S in EXP_ATL (Figure S1b) shows no long-

1 term trend. These results strongly suggest that the increased AMOC strength at 30°S after the
2 1950s in EXP_CTR is not caused by the processes within the Atlantic Ocean. In other words, the
3 AMOC increase at 30°S is pushed from the outside, and not pulled from the inside.

4 Naturally, the next question is why the simulated AMOC at 30°S is strengthened. To answer
5 this question, it is helpful to explore the simulated pathways of the northward heat transport in
6 the Atlantic Ocean. Shown in Figure 3a are the simulated northward heat transport (contours)
7 and heat transport vector (vectors) averaged in the upper 3000m for 1979-2008, obtained from
8 EXP_CTR. It clearly shows that the main pathway of heat transport into the South Atlantic
9 originates from the Indian Ocean in this model. The key roles played in global climate by the
10 Indian-Atlantic inter-ocean exchange have long been recognized¹. The warm water that leaks
11 from the Indian Ocean into the South Atlantic may affect the strength of the AMOC, both on
12 decadal advective time scales and on faster Rossby wave time scales¹⁴. As shown in Figure 3a,
13 the warm water entrained from the Indian Ocean moves northwestward along the South Atlantic
14 subtropical gyre and collides at the western boundary, then continues its northward excursion
15 through the North Brazil Current. The warm water finally arrives at the subpolar Atlantic via the
16 Loop Current, Gulf Stream and North Atlantic Current. The pathways of the heat transport
17 shown in Figure 4a are very similar to the main advective pathway of mass seen in both high-
18 resolution models and surface drifters¹⁵.

19 Figure 3b is identical to Figure 3a except that it shows the difference in the simulated
20 northward heat transport (contours) and heat transport vector (vectors) between 1979-2008 and
21 1871-1900 periods. The pathways of the anomalous northward ocean heat transport are
22 surprisingly similar to those of the mean northward ocean heat transport (Figure 3a). It is clear
23 that the ocean heat transport from the Indian Ocean is increased. This agrees with the observed

1 increase in both upper ocean temperature¹¹ and inter-ocean transport² in the Agulhas region in
2 recent decades. The anomalous anticyclones of the barotropic stream function in the South
3 Atlantic and Indian Ocean between 50°S and 30°S (Figure S2) further indicate that both the
4 South Atlantic subtropical gyre and Indian Ocean subtropical gyre are strengthened. As shown in
5 Figure 3c, this is consistent with the observed westerly wind anomalies over the Southern Ocean
6 and the associated strengthening of the wind stress curl over the region from 50°S to 30°S, as
7 suggested by earlier high- and low-resolution modeling studies^{2,12}. It is important to note that
8 Ekman transport does not directly contribute to the increased AMOC at 30°S since the zonal
9 wind stress at 30°S is nearly unchanged (Figure 3c). Since the westerly wind anomalies over the
10 Southern Ocean are largely linked to the Southern Annular Mode (SAM), it appears that the
11 increased AMOC at 30°S in EXP_CTR is ultimately caused by the increasing trend of the SAM
12 since the mid-20th century. The cause of the SAM trend is not the focus of this study, but one
13 popular hypothesis involves the Antarctic ozone losses with important contributions from
14 increases in anthropogenic greenhouse gases¹³.

15 As summarized schematically in Figure 4, here we show that the observed warming trend of
16 the Atlantic Ocean since the 1950s is largely due to the concurrent increase in the Indian-to-
17 Atlantic inter-ocean heat transport. One potential future work is to use a fully coupled model
18 initialized with EXP_CTR to explore whether the increased buoyancy in the North Atlantic
19 Ocean will eventually lead to decreased North Atlantic deep convection in the 21st century.

20

21

22

23

1 **Methods**

2 **20th Century Reanalysis (20CR).** It is virtually impossible to properly initialize a global ocean
3 model at the mid-20th century due to the paucity of observational hydrographic data for the
4 globe during that period. An alternative approach is to start an ocean model simulation
5 sufficiently earlier than the mid-20th century with an arbitrary set of initial conditions. However,
6 none of the surface-forced ocean model studies so far has been simulated with the surface
7 forcing prior to the mid-20th century because the surface forcing data, which are typically
8 derived from atmospheric reanalysis products such as NCEP-NCAR reanalysis, are limited to the
9 last 50 - 60 years. Recently, the newly developed NOAA-CIRES 20th Century Reanalysis
10 (20CR) has been completed⁴. The 20CR provides the first estimate of global surface momentum,
11 heat and freshwater fluxes spanning the late 19th century and the entire 20th century (1871-
12 2008) at daily temporal and 2° spatial resolutions.

13

14 **CCSM3_POP.** The global ocean-ice coupled model of the NCAR Community Climate System
15 Model version 3 (CCSM3) forced with the 20CR is used as the primary tool in this study. The
16 ocean model is a level-coordinate model based on the Parallel Ocean Program (POP). It solves
17 the three-dimensional primitive equations under hydrostatic and Boussinesq approximations. The
18 ice model, the NCAR Community Sea Ice Model version 5, is a dynamic-thermodynamic ice
19 model that computes local growth rates of sea ice due to vertical conductive, radiative and
20 turbulent fluxes. The ocean model is divided into 25 vertical levels. Both the ocean and ice
21 models have 100 longitudes and 116 latitudes on a displaced pole grid with a longitudinal
22 resolution of 3.6 degrees and a variable latitudinal resolution of approximately 0.9 degrees near
23 the equator¹⁷.

1
2 **CCSM3_POP Spin-up.** To spin up the model, the fully coupled (atmosphere-land-ocean-ice)
3 CCSM3 control experiment is performed for 700 years with pre-industrial climate condition of
4 the 1870s. The 700th year output of the CCSM3 spin-up run is then used to initialize the CCSM3
5 ocean-ice model (CCSM3_POP hereafter), which is further integrated for 200 more years using
6 the daily 20CR surface flux fields for the period of 1871-1900. To incorporate the impact of
7 atmospheric noise, which plays a crucial role in the thermohaline convection and deep-water
8 formation in the North Atlantic sinking regions, during the spin-up, the surface forcing fields in
9 each model year are alternated with those of a randomly selected year from 1871 to 1900. In the
10 200 years of the CCSM3_POP spin-up run, the simulated AMOC and associated heat transport
11 show no sign of drift after about 150 years. Nevertheless, the 900 years of spin-up may not be
12 long enough for deep oceans to reach a quasi-equilibrium state, if there is any. Therefore, the
13 CCSM3 spin-up run is continued for additional 138 years, which is referred to as the reference
14 run, then subtracted from the real-time runs, which are described below, for each model year to
15 cancel out any potential long-term model drift.

16
17 **CCSM3_POP experiments.** After the total of 900 years of spin up runs, three model
18 experiments are performed. In the control experiment (EXP_CTR), the CCSM3_POP is
19 integrated for 1871-2008 using the real-time daily 20CR surface flux fields. The next two
20 experiments are idealized experiments designed to understand the Atlantic Ocean heat content
21 change with and without the influence of the northward heat transport change at 30°S. The
22 remote ocean warming experiment (EXP_REM) is identical to EXP_CTR except that the surface
23 forcing fields north of 30°S are from the daily 20CR surface flux fields for the period of 1871-

1 1900 exactly like the spin-up experiment, whereas those south of 30°S are real time as in
2 EXP_CTRL. The Atlantic Ocean warming experiment (EXP_ATL) is also identical to EXP_CTRL
3 except that the surface forcing fields south of 30°S are from the daily 20CR surface flux fields
4 for the period of 1871-1900 as in the spin-up experiment, whereas those north of 30°S are real
5 time as in EXP_CTRL. Note that the Atlantic Ocean warms only through anomalous surface
6 warming in EXP_ATL, and only through anomalous northward ocean heat transport at 30°S in
7 EXP_REM, respectively.

8
9 **Acknowledgments.** This study was motivated and benefited from the AMOC discussion group
10 of the research community at UM/RSMAS and NOAA/AOML. We acknowledge helpful
11 suggestions from Ping Chang. This work was supported by grants from the NOAA and NSF.

12

13 **References**

- 14 1. Biastoch, A., Böning, C. W. & Lutjeharms, J. R. E. Agulhas leakage dynamics affects
15 decadal variability in Atlantic overturning circulation, *Nature*, **456**, 489–492 (2008).
- 16 2. Biastoch, A., Böning, C. W. Schwarzkopf, F. U. & Lutjeharms, J. R. E. Increase in Agulhas
17 leakage due to poleward shift in the southern hemisphere westerlies, *Nature*, **462**,
18 doi:10.1038/nature08519, 495-498 (2009).
- 19 3. Broecker, W. S. The biggest chill, *Natural History*, **96**, 74-82 (1987) .
- 20 4. Compo, G.P., *et al.* The twentieth century reanalysis project. *Quarterly J. Roy. Meteorol.*
21 *Soc.*, **137**, 1-28. doi: 10.1002/qj.776 (2011).
- 22 5. Lee, S.-K., Enfield, D. B. & Wang, C. Future impact of differential inter-basin ocean
23 warming on Atlantic hurricanes. *J. Climate*, **24**, 1264-1275 (2011).

- 1 6. Levitus, S., Antonov, J. I. Boyer, T. P. & Stephens, C. Warming of the world ocean. *Science*
2 **287**, 2225-2229, doi:10.1126/science.287.5461.2225 (2000).
- 3 7. Levitus, S., Antonov, J. I. Wang, J. Delworth, T. L. Dixon, K. W. & Broccoli, A. J.
4 Anthropogenic warming of earth's climate system, *Science* **287**, 2225-2229,
5 doi:10.1126/science.287.5461.2225 (2001).
- 6 8. Levitus, S., Antonov, J. I. Boyer, T. P. Locarnini, R. A. Garcia, H. E. & Mishonov, A. V.
7 Global ocean heat content 1955–2008 in light of recently revealed instrumentation problems,
8 *Geophys. Res. Lett.*, **36**, L07608, doi:10.1029/2008GL037155 (2009) .
- 9 9. Lozier, M. S., Roussenov, V. Mark, S. Reed, C. & Williams, R. G. Opposing decadal
10 changes for the North Atlantic meridional overturning circulation. *Nature Geosci.* **3**, 728-
11 734 (2010).
- 12 10. Lumpkin, R. & Speer, K. Global ocean meridional overturning. *J. Phys. Oceanogr.*, **37**,
13 2550-2562 (2007).
- 14 11. Rouault, M., Penven, P. & Pohl, B. Warming in the Agulhas Current system since the
15 1980's, *Geophys. Res. Lett.*, **36**, L12, 602 (2009).
- 16 12. Sijp, W. P., & England, M. H. Southern hemisphere westerly wind control over the ocean's
17 thermohaline circulation. *J. Climate*, **22**, 1277-1286 (2009).
- 18 13. Thompson, D. W. & Solomon, S. Interpretation of recent southern hemisphere climate
19 change, 296, 895-899, doi:10.1126/science.1069270 (2002).
- 20 14. Van Sebille, E., & Van Leeuwen, P. J. Fast northward energy transfer in the Atlantic due to
21 Agulhas rings, *J. Phys. Oceanogr.*, **37**, 2305–2315 (2007).

- 1 15. Van Sebille, E., Beal, L. M. & Johns, W. E. Advective time scales of Agulhas leakage to the
2 North Atlantic in surface drifter observations and the 3D OFES model, *J. Phys. Oceanogr.*,
3 in press (2011).
- 4 16. Xie, S.-P., Deser, C. Vecchi, G. A., Ma, J. Teng, H. & Wittenberg, A. T. Global warming
5 pattern formation: Sea surface temperature and rainfall. *J. Climate*, 23, 966-986 (2010).
- 6 17. Yeager, S. G., Shields, C. A. Large, W. G. & Hack, J. J. The low-resolution CCSM3. *J.*
7 *Climate*, **19**, 2545-2566 (2006).

8
9
10
11
12
13
14
15
16
17
18
19
20
21
22
23

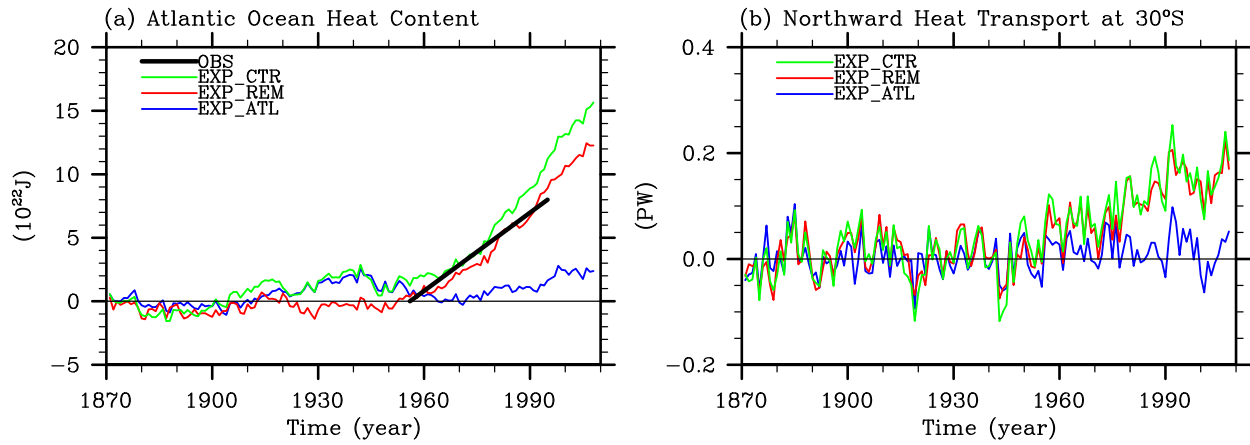
1 **Figure 1.** (a) Simulated Atlantic Ocean heat content changes in the upper 3000m and (b)
2 northward ocean heat transports in the South Atlantic at 30°S in reference to 1871-1900 obtained
3 from the three model experiments. The thick black line in (a) is the observed trend of the Atlantic
4 Ocean heat content increase⁶.

5
6 **Figure 2.** (a) Time-averaged AMOC during 1979-2008 and (b) time series of the AMOC index
7 (maximum overturning stream function) at 30°S obtained from EXP_CTRL.

8
9 **Figure 3.** (a) Simulated pathways of the northward heat transport (contours) and heat transport
10 vector (vectors) averaged in the upper 3000m for 1979-2008, obtained from EXP_CTRL. The unit
11 is K·cm/sec. (b) The difference in the simulated northward heat transport (contours) and heat
12 transport vector (vectors) between 1979-2008 and 1871-1900 periods, obtained from EXP_CTRL.
13 (c) Globally averaged zonal wind stress for 1871-1900 and for 1979-2008 periods, obtained from
14 the 20CR.

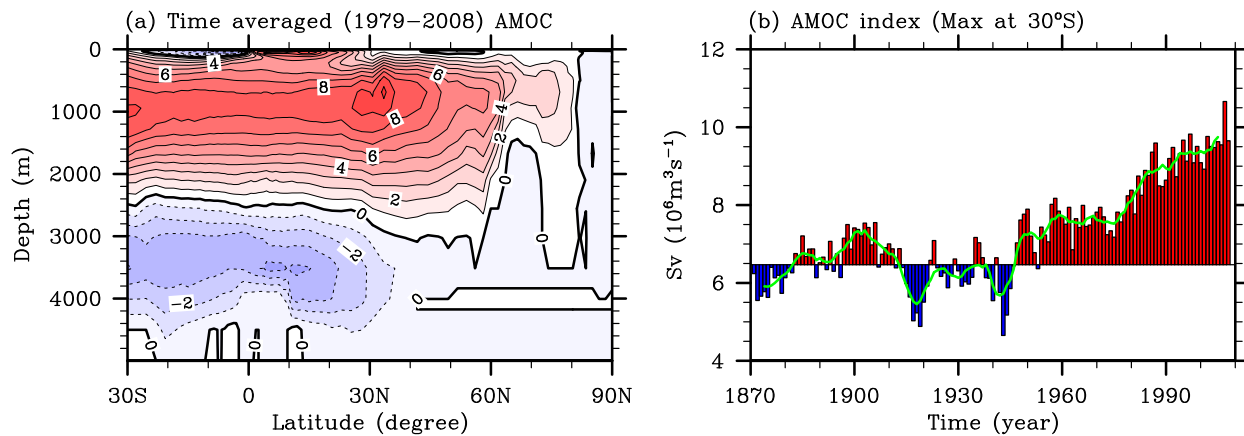
15
16 **Figure 4.** This schematic drawing illustrates that the observed warming trend of the Atlantic
17 Ocean since the 1950s is largely due to the concurrent increase in the Indian-to-Atlantic inter-
18 ocean heat transport. The subpolar North Atlantic Ocean was slightly cooled during the 1950s-
19 1990s⁹.

20
21



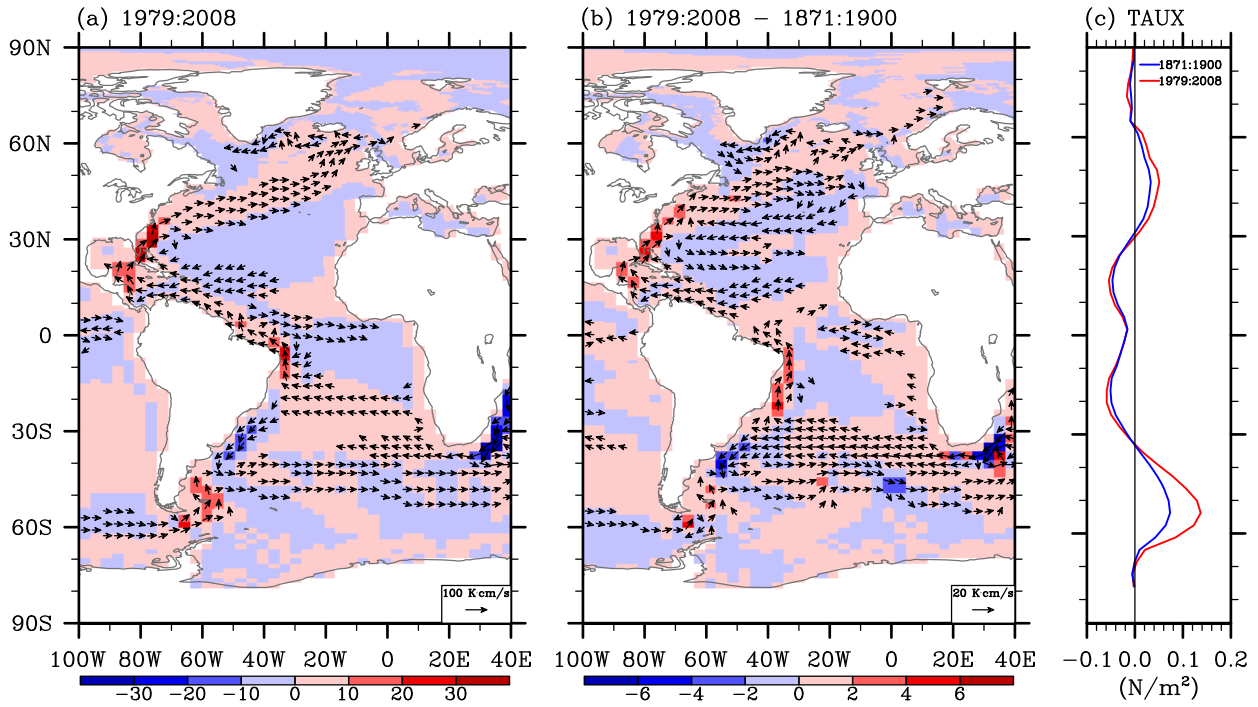
1
 2 **Figure 1.** (a) Simulated Atlantic Ocean heat content change in the upper 3000m and (b)
 3 simulated northward ocean heat transport in the South Atlantic at 30°S in reference to 1871-1900
 4 obtained from the three model experiments. The thick black line in (a) is the observed trend of
 5 the Atlantic Ocean heat content increase⁶.

6
 7
 8
 9
 10
 11
 12
 13
 14
 15
 16
 17



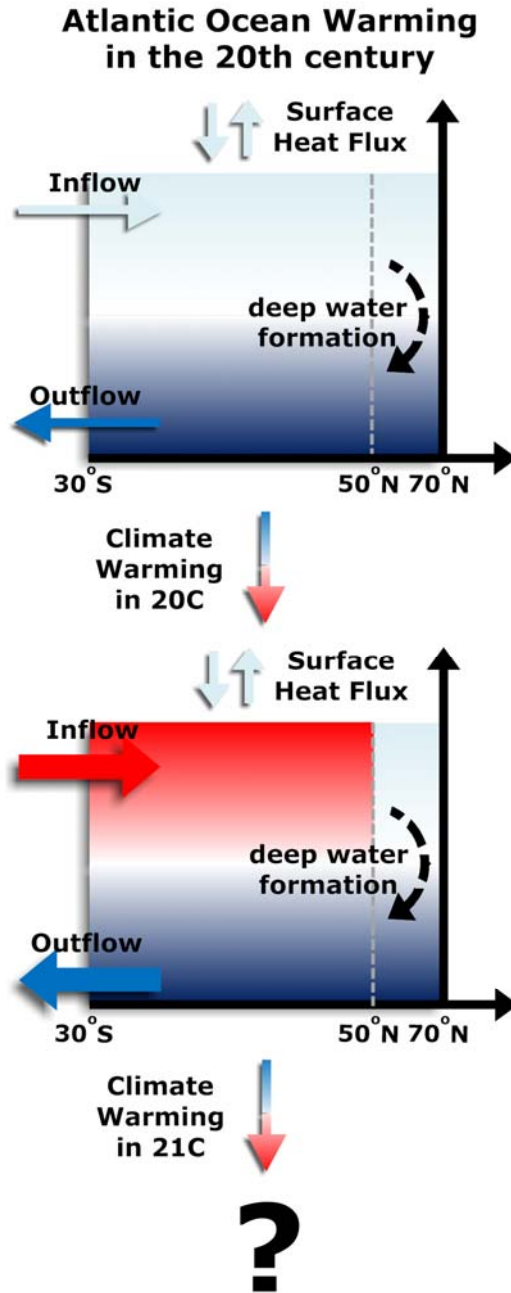
1
2 **Figure 2.** (a) Time-averaged AMOC during 1979-2008 and (b) time series of the simulated
3 AMOC index (maximum overturning stream function) at 30°S obtained from EXP_CTR.

4
5
6
7
8
9
10
11
12
13
14
15
16
17



1
2 **Figure 3.** (a) Simulated pathways of the northward heat transport (contours) and heat transport
3 vector (vectors) averaged in the upper 3000 m for 1979-2008, obtained from EXP_CTR. The
4 unit is K·cm/sec. (b) Differences in the simulated northward heat transport (contours) and heat
5 transport vector (vectors) between 1979-2008 and 1871-1900 periods, obtained from EXP_CTR.
6 (c) Globally averaged zonal wind stress for 1871-1900 and for 1979-2008 periods, obtained from
7 the 20CR.

8
9
10
11
12
13



1

2 **Figure 4.** This schematic drawing illustrates that the observed warming trend of the Atlantic

3 Ocean since the 1950s is largely due to the concurrent increase in the Indian-to-Atlantic inter-

4 ocean heat transport. The subpolar North Atlantic Ocean was slightly cooled during the 1950s-

5 1990s in both observations⁹ and EXP_CTR (Figure S3).

6